Geology of Ore Deposits, Vol. 46, No. 5, 2004, pp. 332–352. Translated from Geologiya Rudnykh Mestorozhdenii, Vol. 46, No. 5, 2004, pp. 385–406.

Minerals and Formation Conditions of Ores of the Teremkin Gold Deposit (Eastern Transbaikal Region, Russia)

V. Yu. Prokof'ev*, [1], L. D. Zorina, I. A. Baksheev***, O. Yu. Plotinskaya*, O. E. Kudryavtseva***, and Yu. M. Ishkov******

**Institute of Geology of Ore Deposits, Petrography, Mineralogy, and Geochemistry (IGEM), Russian Academy of Sciences, Staromonetnyi per. 35, Moscow, 119017 Russia*
***Vinogradov Institute of Geochemistry and Analytical Chemistry, Siberian Division, Russian Academy of Sciences, ul. Favorskogo 1a, Irkutsk, 664033 Russia*
****Moscow State University, Vorob'evy gory, Moscow, 119899 Russia*
*****Institute of Geology, Siberian Division, Russian Academy of Sciences, ul. Sakh'yanovoi 6, Ulan-Ude, 670047 Russia*

Received May 18, 2004

Abstract—Physicochemical conditions of the formation of ores from the Teremkin gold deposit have been reconstructed on the basis of comprehensive studies of fluid inclusions and chemical compositions of principal minerals of ore veins: tourmaline, mica, carbonate, gold, sphalerite, and galena. The hydrothermal process at the Teremkin deposit was established to proceed at temperatures of 466…118°C and pressures of 410…70 bar on the background of a heterogeneous state of the ore-forming fluids and elevated oxidizing potential at the beginning of the hydrothermal process. Productive mineralization formed at temperatures of 297…216°C and pressures of 160…70 bar. The concentration of salts in fluids varied from 34.7 to 1.2 wt %-equiv. NaCl. Basic fluid components are represented by sodium and calcium chlorides, carbon dioxide, and boron. High concentrations of boron in ore-forming fluid of the Teremkin deposit and values of the ratios K/Rb, Sr/Rb, Ba/Rb, Sr/Ba, and Ni/Co in the fluid of inclusions indicate its magmatic nature and the magmatic source of some elements in ores. Physicochemical parameters of the formation of the object of study have been compared to those of the Darasun deposit. The small scale of gold mineralization at the Teremkin deposit is accounted for, first of all, by a short-term ore-forming process.

INTRODUCTION

The Teremkin deposit is located within the Eastern Transbaikal region (Fig. 1), near the settlement of Vershino-Darasunskii. It is 5 km northwest of the large Darasun deposit (Fig. 2) and, along with it, forms part of a single ore–magmatic system; i.e., spatially and paragenetically, it is related to the same granodiorite–porphyry intrusion as the Darasun deposit (Timofeevskii, 1972). The Teremkin deposit is small, although the gold content in its ores is very high and easily recoverable. That is why, in the recent years of economic recession, when the Darasun deposit was temporarily closed down because most gold reserves in it are related to sulfides and thus a complicated technological process is required for gold recovery, the development of the Teremkin deposit was still in progress. Some features of the geological structure of the Teremkin deposit and its the geochemical zonation have already been described in a series of works (Gulina, 1988; Kulikova and Zorina, 1989, 1999; Zorina *et al.*, 1991; Yurgenson and Yurgenson, 1995; Kulikova *et al.*, 1996; and others). However, the chemical composition of the Teremkin deposit and its conditions of ore formation have not been adequately studied to correlate these data with those for the Darasun deposit (Sakharova, 1968, 1972; Timofeevskii, 1972; Prokof'ev and Zorina, 1994, 1996; Prokof'ev *et al.*, 2000). Such a correlation at the modern comprehensive level of investigation is important in the context of studying the genesis of large gold deposits. To understand factors responsible for the scale of mineralization of deposits similar in genesis, the comparative analysis of formation conditions for large and small deposits is required. Conditions of formation for large deposits have been studied in detail (Konstantinov *et al.*, 2000, and others), but no such data are available for small deposits. For this reason, to reconstruct the physicochemical parameters of ore deposition at the Teremkin deposit, we studied the compositions of main ore minerals and mineral-forming fluids, as well as assessed parameters of ore formation, and correlated the data obtained with the information on the Darasun deposit.

BRIEF CHARACTERISTICS OF THE DEPOSIT

The Teremkin deposit consists of a series of gentle (predominating) and steeply dipping tourmaline–quartz–sulfide veins with commercial gold mineraliza-

[1]Corresponding author: V.Yu. Prokof'ev. E-mail: vpr@igem.ru

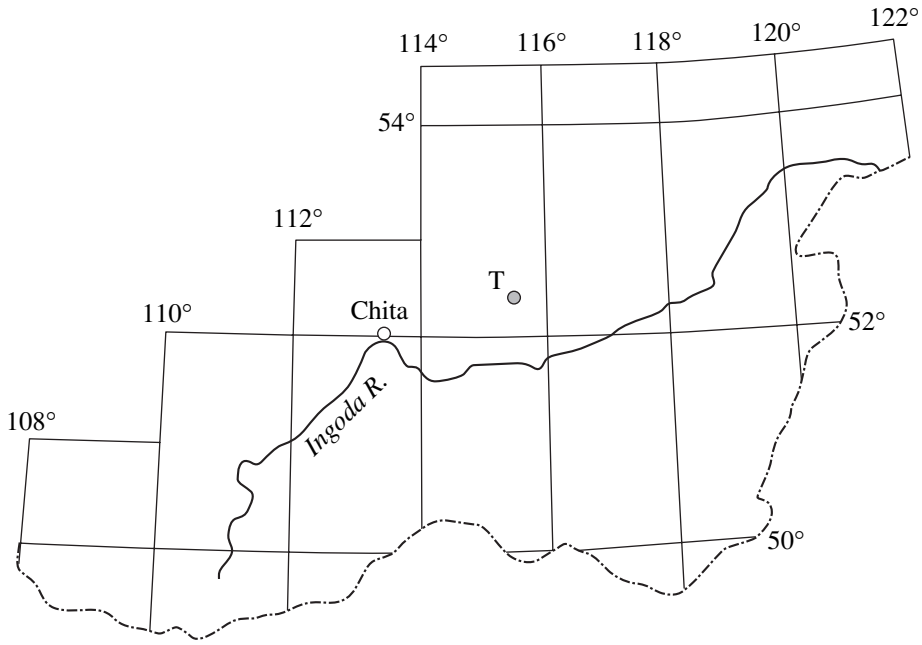

Fig. 1. Geographical position of the Teremkin deposit (T, deposit).

tion, as well as noncommercial mineralization zones (Fig. 3). Gold in ores is visible. In addition to gold, reserves of Ag, Cu, and Bi have also been assessed. Recovered from concentrate are Au, Ag, Cu, Bi, Pb, Zn, Sb, and other elements. Host rocks are represented by Early Paleozoic gabbroids and Middle Paleozoic–Early Mesozoic granitoids. The structure of the deposit is defined by the intersection of gentle (20°), potassium-rich granodiorite porphyry, plagioporphyry, felsite, felsite porphyry, and volcanic glass dikes of Mesozoic age, trending northwestward, with a system of northeast- and north–south-trending gentle and steep faults. Volcanic glass and felsite are characterized by an anomalously high boron content (up to 295 g/t in green glass, up to 180 g/t in brown glass, and up to 325 g/t in felsite) compared to glass from other volcanic structures of the Transbaikal region (Antipin *et al.*, 1985). Dikes serve as screens forming a multilevel structure of the deposit. There are three levels known at present. Orebodies are localized below dike screens. Faults represent channelways and localizing structures for ore.

The distinguishing features of ore mineralization at the Teremkin deposit are an extremely irregular distribution of gold and the occurrence of clearly defined ore shoots. Main gold reserves are concentrated in northeast-trending, steeply (50°) dipping southward veins, as well as in gently (10°–30°) dipping southward or northeastward veins. Ore shoots occur in vein swellings confined to areas of fissure intersection, conjunction, and branching. The most favorable areas for ore shoots are the conjunctions of tectonic dislocations: WE-, NE-, and NS-trending structures. Main reserves of high-grade ores are found at the conjunction of tectonic structures and gently dipping dikes. Explosive breccias were described in which ores are also localized (Kulikova *et al.*, 1996).

Special works on the mineralogy of the Teremkin deposit are unavailable. The published works (Zorina *et al.*, 1991; Yurgenson and Yurgenson, 1995) report that ores comprise quartz, tourmaline (Fig. 4a), pyrite, arsenopyrite, chalcopyrite, sphalerite (Fig. 4b), galena, marcasite, pyrrhotite, gray ore, native gold (Fig. 4c), electrum, bismuth minerals (native bismuth, bismuthine, aikinite (Fig. 4d), cosalite, and tetradymite), bournonite and other lead sulfoantimonites, carbonate, chalcedony, zeolite, and fluorite. No analyses of the chemical compositions of minerals from the Teremkin deposit are available in published works except the composition of tourmaline (Afonina *et al.*, 1990). When studying the compositions of ore minerals with an X-ray spectrographic microanalyzer, we revealed matildite $AgBiS_2$ in association with galena (Fig. 4c), which was not found before at the deposit. The mineralogy of the Darasun deposit is more diverse compared to the Teremkin deposit (Timofeevskii, 1972, and others), although all minerals known in the latter are found in the former.

The history of the hydrothermal activity at the Teremkin deposit was complicated, and it was described by Zorina *et al.* (1991). Prior to the formation of gold-bearing veins, massive milky white quartz veins and rare quartz–molybdenite veins formed. Intense spatial propylitic alteration of ore-hosting rocks, which precedes the formation of gold-bearing veins, was found (Kulikova and Zorina, 1989; Zorina *et al.*, 1991). By analogy with the Darasun deposit (Prokof'ev and

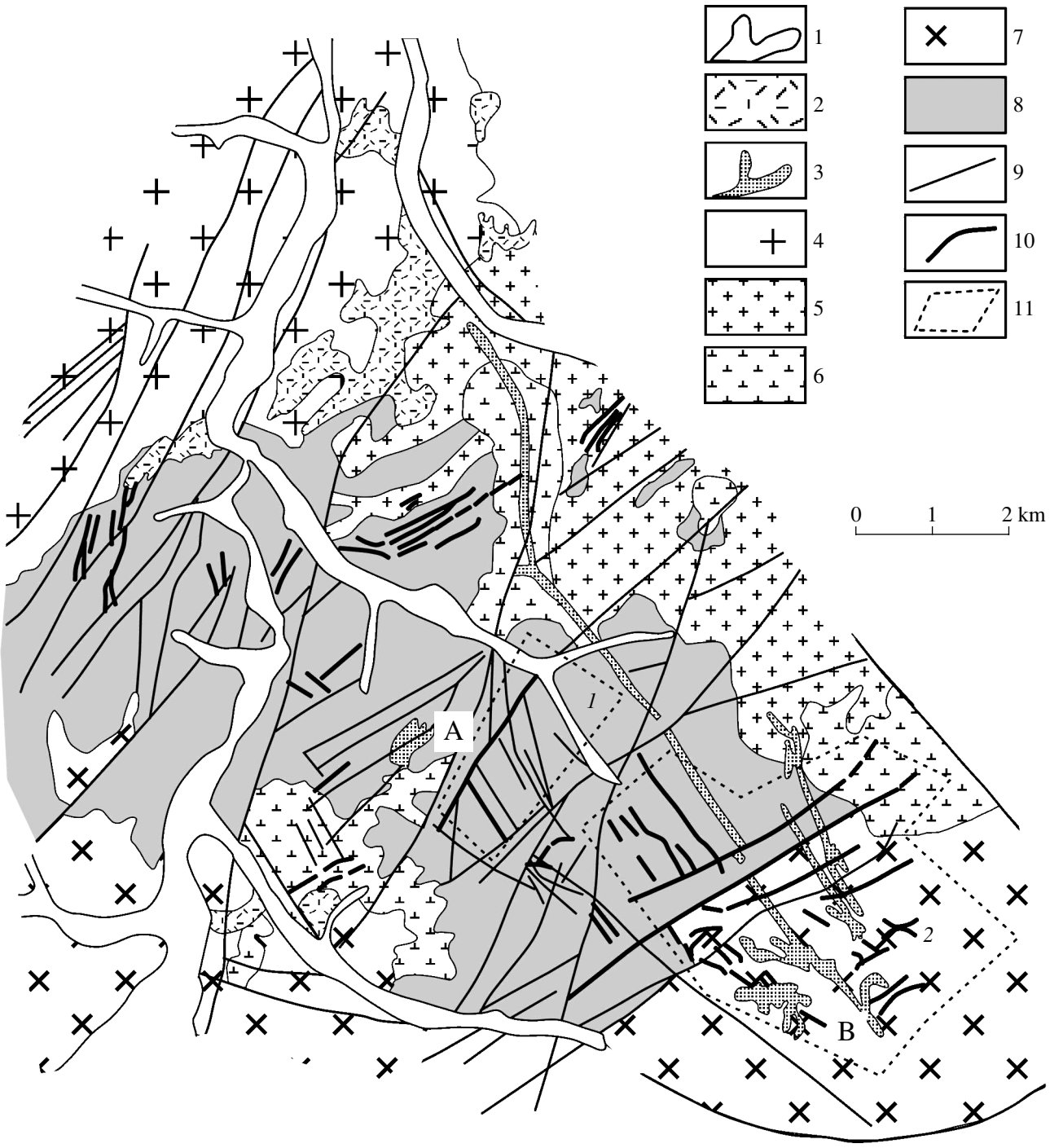

Fig. 2. Geological map of the Darasun ore field (based on materials of the Darasun Geological Prospecting Expedition). (1) Alluvial deposits; (2, 3) Amudzhikan–Sretensk complex (J_{2-3}): (2) volcanics; (3) subvolcanic and dike bodies of porphyric rocks: dioritic porphyrite, granodiorite porphyry, granite porphyry, and others (A—Ring anomaly, B—Darasun carcass intrusion); (4) Amanan complex (T): biotite-hornblende granites, granodiorites; (5, 6) Olekma complex (PZ_3–MZ_1): (5) biotitic and leucocratic granites; (6) syenite, granosyenite, quartz syenite; (7) Kresty complex (PZ_2): diorite, quartz diorite, granodiorite; (8) Kruchinin complex of metamorphosed gabbroid rocks (PZ_1): granitized gabbro, amphibolite, gabbrodiorite, troctolite; (9) tectonic dislocations; (10) ore bodies; (11) deposits: *1*—Teremkin, *2*—Darasun.

Zorina, 1996), we have distinguished three stages (I–III) in the formation of mineral assemblages of ore veins: (I) preore (successive mineral paragenetic assemblages quartz–tourmaline–pyrite and quartz–arsenopyrite–chalcopyrite), (II) productive (quartz–pyrite–chalcopyrite–gold, quartz–chalcopyrite–sphalerite–galena–gold, galena–matildite–gold, quartz–gray ore–chalcopyrite–gold–electrum–pyrrhotite, and quartz–calcite–bourno-

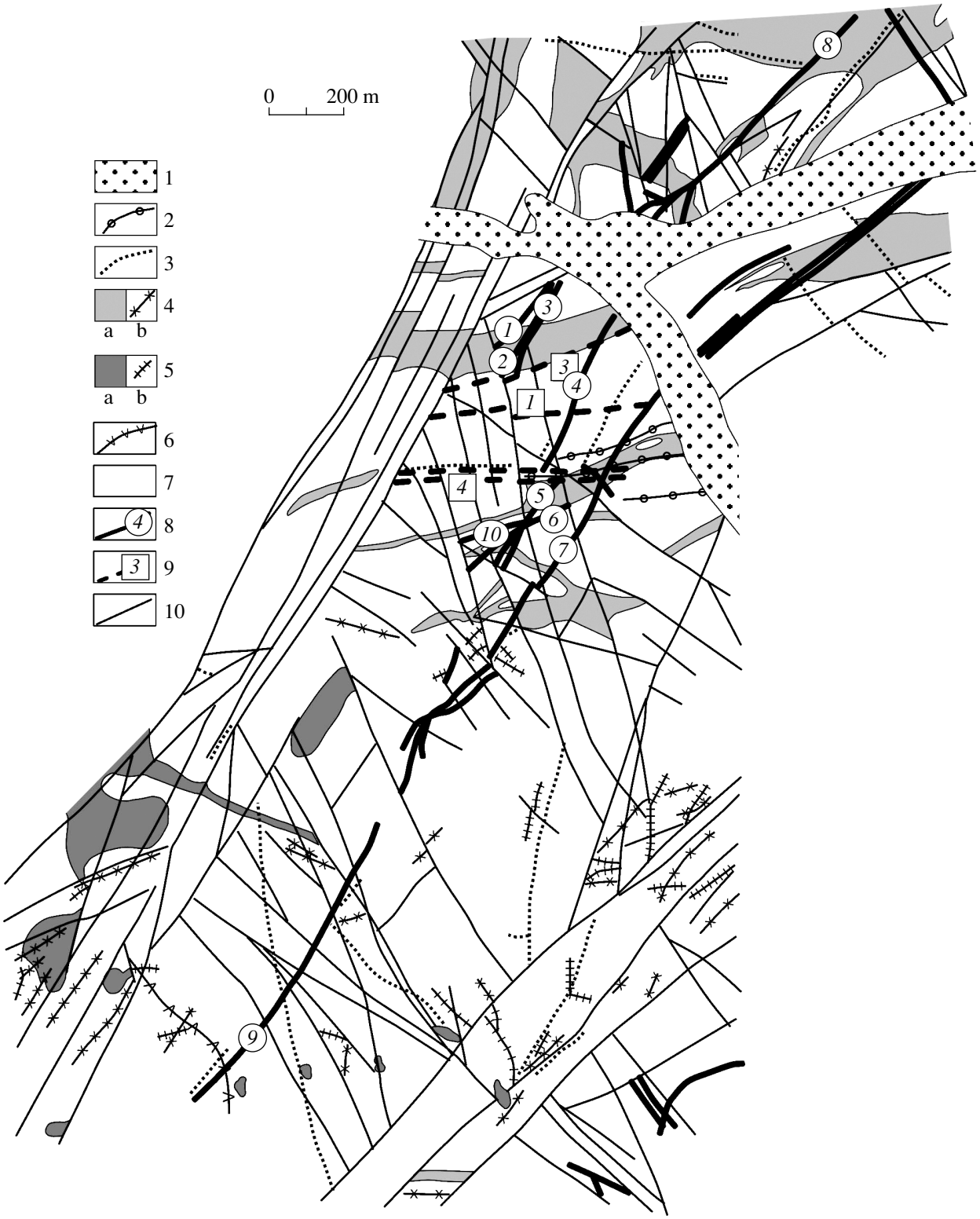

Fig. 3. Geological map of the Teremkin deposit (compiled on the basis of geological survey, prospecting, and exploration carried out by Yu.A. Aferov, N.M. Kalinichenko, N.T. Konovalova, A.V. Eletskii, V.I. Minin, R.A. Amosov, and I.B. Semerkov). (1) Quaternary deposits; (2) dikes of dioritic porphyrite (J_{2-3}); (3) dikes of plagioporphyry, plagiogranodiorite porphyry, felsite porphyry, felsite, volcanic glass (J_{2-3}); (4) leucocratic granite and biotitic granite (a) and their dike facies (b) (PZ_2–MZ_1); (5) syenite and quartz syenite (a) and their dike facies (b) (PZ_2–MZ_1); (6) microgabbro dike (PZ_2–MZ_1); (7) metamorphosed and granitized gabbro, gabbrodiorite, pyroxene, gabbro–diabase (PZ_1); (8) ore veins and their numbers (*1*—Severnaya, *2*—Vesennyaya, *3*—Okhristaya, *4*—Gornyatskaya, *5*—Skorostnaya, *6*—Pologaya, *7*—Postnaya, *8*—Zolushka, *9*—Zagadochnaya, *10*—vein 2); (9) ore zones and their numbers; (10) tectonic dislocations.

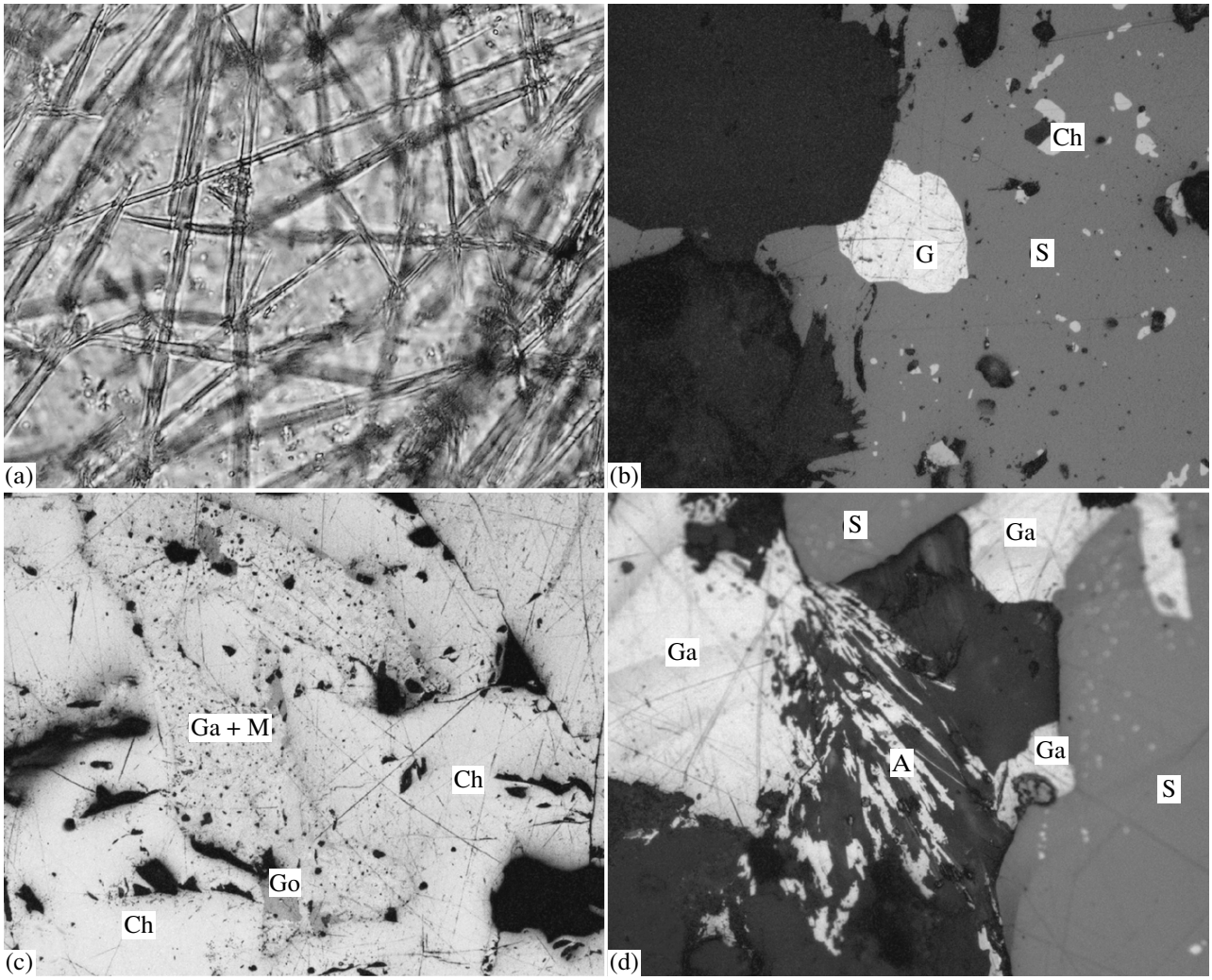

Fig. 4. Minerals of ore veins of the Teremkin deposit. (a) Tourmaline crystals in quartz; (b) gold in sphalerite with emulsion dissemination of chalcopyrite; (c) galena–matildite aggregate with fahlores in chalcopyrite; (d) acicular crystals of aikinite-like mineral in carbonate. G—gold, S—sphalerite, Ch—chalcopyrite, Ga—galena, M—matildite, Go—fahlores, A—aikinite.

nite–native bismuth–bismuthine–aikinite–galena–cosalite–tetradymite–gold assemblages), and (III) postore (quartz–carbonate assemblage).

Gold grains are round (Fig. 4c); as large as 50 μm; with gradual boundaries; and with quartz, chalcopyrite, sphalerite, galena, and bismuth minerals in intergrowths. In some veins, quartz–tourmaline and quartz–pyrite assemblages are replaced from selvages to the center by quartz–sulfide assemblages with gold and quartz–carbonate aggregates in the vein center. Broken quartz–tourmaline and pyrite fragments are often cemented by sulfides. The formation of productive veins was accompanied by quartz–sericite–carbonate and chlorite–carbonate–talc alteration of host rocks (the Rb–Sr age of wallrock metasomatites is 145 Ma (Pakhol'chenko *et al.*, 1987), i.e., a bit younger than metasomatites of the Darasun deposit—165 Ma (Timofeevskii, 1972)).

INVESTIGATION METHODS

Chemical compositions of minerals were established with a Camebax SX-50 X-ray spectrographic microanalyzer (Moscow State University, Department of Mineralogy, analyst N.N. Kononkova). Conditions of the analysis were as follows: current of the probe, 30 nA; accelerating voltage, 15 kV; and diameter of the beam, about 3 μm. The following minerals and compounds were used as standards in analyzing tourmaline and mica: hornblende for basic components (Si, Al, Ca, Mg, and Fe), orthoclase for K, albite for Na, fluorophlogopite for F, $MnTiO_3$ for Mn and Ti, vanadite for V, NiO for Ni, and Cr_2O_3 for Cr; in analyzing carbonates: wollastonite for Ca, hypersthene for Mg and Fe, pyrophanite for Mn, and celestine for Sr. Measurements were carried out using the following analytical lines: SiK_α, AlK_α, CaK_α, MgK_α, FeK_α, KK_α, NaK_α, FK_α, MnK_α, TiK_α, VK_α, NiK_α, and CrK_α. The receptiveness of the device was 0.02%, and the telemetry

error was ±2% for basic components and about 20% for admixtures elements. PAP corrections were used for the correcting procedure.

Tourmaline was also analyzed with a JCXA-733 X-ray spectrographic microanalyzer (Institute of Geochemistry SD RAS; analyst, Yu.D. Bobrov). The accelerating voltage was 15 kV, and the current of the probe, 15 mA. Standards were albite (for Na, Al), orthoclase (for K, Si), diopside (for Mg, Ca), pyrope (for Fe), and TiO_2 (for Ti). Intensities were automatically calculated by the ZAF method.

The compositions of ore minerals were studied with a Camebax microbeam X-ray spectrographic microanalyzer (Institute of Geochemistry and Analytical Chemistry, Russian Academy of Sciences (GEOKhI RAS); analyst, N.N. Kononkova). The accelerating voltage was 20 kV, and the current of the probe, 30 mA. Standards in analyzing galena were PbS (for Pb, S), Bi (for Bi), and Ag (for Ag); in analyzing sphalerite, ZnS (for Zn, S), FeS_2 (for Fe), and pure metals (for Cd, Mn, Cu); and, in analyzing gold, pure metals (for Au, Ag, Cu) and HgS (for Hg and S). Measurements were carried out using the following analytical lines: PbM_α, SK_α, BiM_α, AgL_α, AuL_α, ZnK_α, FeK_α, CdL_α, MnK_α, CuK_α, HgL_α, and SeL_α. The beam diameter was 2–5 μm.

Microthermometry of fluid inclusions. For microthermometric studies, we used a measuring system elaborated on the basis of a THMSG-600 microthermocamera (Linkam Company, United Kingdom); an Amplival microscope (Germany) provided with a set of long-focus lenses, including an 80^x lens (Olympus, Japan; video cameras; and a controlling computer. The system allows measurement of temperatures of phase transitions within the interval from –196 to 600°C in real time, their observation at high magnifications, and taking of electronic microphotographs. The concentration of salts in inclusions without solid gases was assessed by the temperature of ice melting ($T_{\text{ice melt}}$) using data from the work by Bodnar and Vityk (1994). The pressure was determined for a heterogeneous fluid based on syngenetic vapor-rich and liquid-vapor inclusions as the sum of the water vapor pressure and the CO_2 pressure. Salt concentrations and vapor and CO_2 pressures were assessed by using the program FLINCOR (Brown, 1989).

Gas chromatography. The compositions of fluid inclusions were studied by chromatographic methods. Gas components and water were analyzed with a Tsvet100M gas chromatograph, model 163. The scheme of the setup and methods of assessment are described by Mironova *et al.* (1992). Sensitivity of the analysis of gas components (μl) was 0.1 for N_2, 4×10^{-2} for CH_4, 3×10^{-2} for CO_2, and 5×10^{-5} for H_2O.

Ion chromatography. Anion compositions were studied at GEOKhI RAS by the method of ion chromatography (Savel'eva *et al.*, 1988). The elutriating agent used eliminated the possibility of establishing bicarbonate ion. Inclusions were unsealed by the thermal method with heating up to 380°C (Savel'eva and Naumov, 1980). Samples were decrepitated in quartz shells in a vacuum system with a liquid manometer, and the total volume of gases and water liberated on unsealing the inclusions was calculated by the growth of pressure in the vacuum system, after which water was absorbed by P_2O_5 and the volume of gases was assessed by the pressure drop (Naumov *et al.*, 1983). A decrepitated specimen in the same quartz shell was covered with twice-distilled water in the proportion 1 : 1 and stirred for about 10 min for complete dissolution of salt components removed from inclusions upon unsealing. Then the extract was decanted and its anion composition was analyzed by the method of ion chromatography. Concentrations of anions in the solution were calculated for a water quantity determined from the same specimen. Results of parallel measurements showed a good reproducibility of the analysis (±15 rel %).

Analysis of liquid extracts from fluid inclusions by the ICP MS method. The analysis of liquid extracts from inclusions by the method of inductively coupled plasma (ICP MS) was carried out from 0.5-g specimens of the 0.5–0.25 mm fraction at the Central Institute of Geological Exploration for Base and Precious Metals (analysts, Yu.V. Vasyuta and A.Yu. Smolenkova) according to the procedure published by Kryazhev *et al.* (2003). Prior to this, in inclusions of the same specimen, the water content was assessed to calculate concentrations of elements in the hydrothermal solution. CO_2 and methane were also analyzed, and, after extract preparation, chlorine, potassium, sodium, calcium, magnesium, dissolved silica, and all the elements that had been detected by the ICP MS method were analyzed.

Laser spectral analysis of individual fluid inclusions. The analysis of individual inclusions by atomic emission spectroscopy with laser unsealing of fluid inclusions (Ishkov and Reif, 1990) was carried out at the Institute of Geology, Siberian Division, Russian Academy of Sciences (Ulan-Ude). The accuracy of the analysis was ±30%.

COMPOSITIONS OF ORE MINERALS

Mineral aggregates formed during the tourmaline stage make up veins and veinlets, as well as enter into the composition of complex gold ore veins.

Tourmaline forms thin acicular black crystals (Fig. 4a) 2 mm long and their intergrowths. The mineral shows pleochroism from light yellow to dark green color, which indicates the presence of Fe^{2+} and Fe^{3+} ions in it. No zonation was found in tourmaline during optical observations. The X-ray spectrographic microanalysis of ingrowths in tourmaline showed that they are represented by quartz, apatite, zircon, and rutile. In chemical compositions, tourmaline corresponds to highly ferrous dravite–schorl–"oxyschorl" with a fluorine content of up to 0.18 wt % and an iron

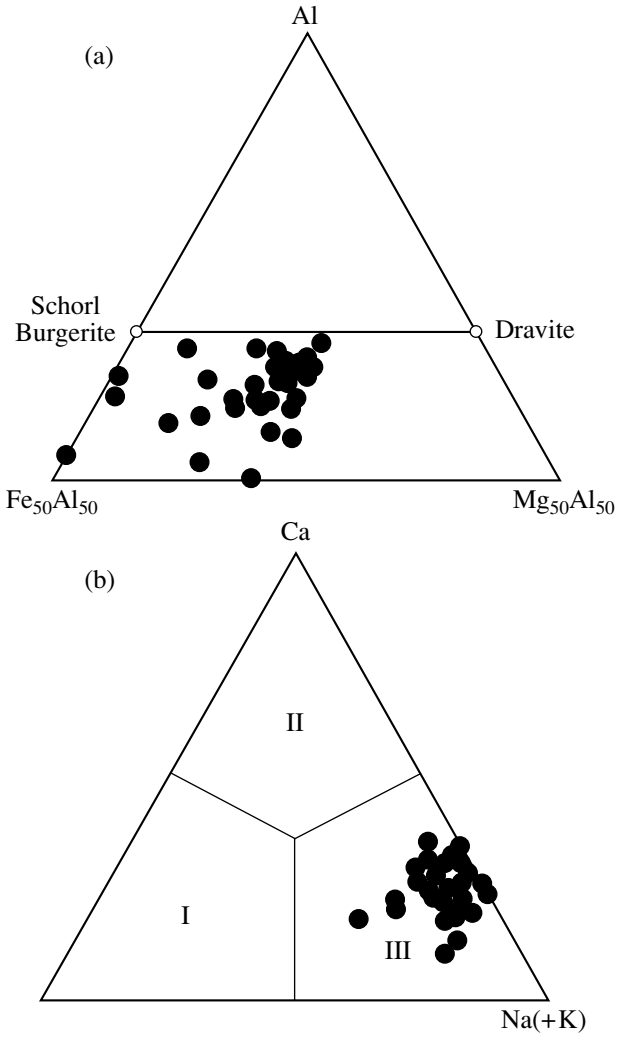

Fig. 5. Ratio of cations of Fe–Al–Mg (a) and □–Ca–Na(+K) (b) in tourmalines of the Teremkin deposit.

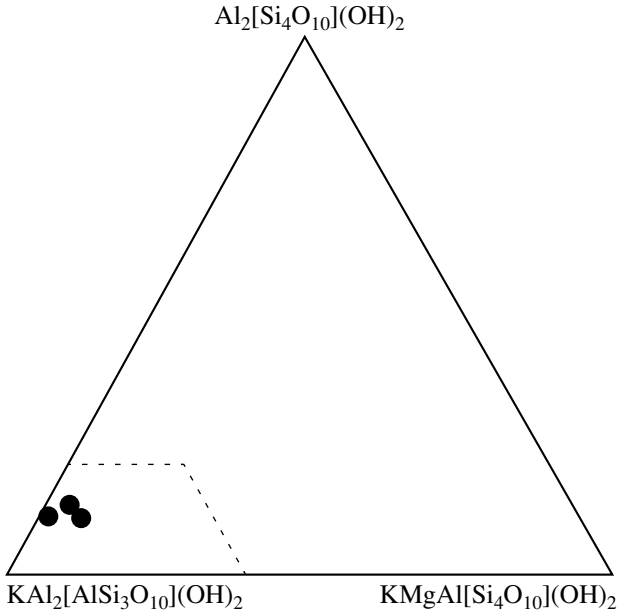

Fig. 6. Chemical compositions of muscovite from tourmaline-bearing quartz veins of the Teremkin deposit. Contour shows the area of muscovite compositions from berezite and listvenite of the Berezovsk gold deposit, Central Urals (Baksheev *et al.*, 1999).

content ($f = Fe_\Sigma \times 100\%/(Fe_\Sigma + Mg)$) of 49.1…83.3% (Table 1). The Ti content makes up 0.12…0.63 wt % TiO_2. The content of TiO_2 decreases (from 0.57 to 0.20 wt %) on going from the crystal center to the edges, whereas the concentration of Na_2O increases (from 1.85 to 2.03 wt %). Concentrations of Cr_2O_3 are 0.10…0.00; V_2O_3, 0.10…0.00; and NiO, 0.13…0.00 wt %. Figurative points of the chemical compositions of tourmaline lie in the diagram $Fe_{50}Al_{50}$–Al–$Mg_{50}Al_{50}$ below the line schorl–dravite (Fig. 5a), indicating indirectly that most iron in the mineral occurs in the form of Fe^{3+} (Slack, 1996). Occurrence of Fe^{3+} is confirmed by the results of some chemical analyses and X-ray studies (Afonina *et al.*, 1990). The ratio Fe^{3+}/Fe_Σ in tourmaline varies from 0.13 to 0.88, averaging 0.5. That is why the contents of Fe^{2+} and Fe^{3+} were calculated in Table 1 on the basis of these data. According to X-ray (powder pattern) data, we may infer that part of Fe^{+3} is in the octahedral position *Z*, replacing Al (Afonina *et al.*, 1990). A high Fe^{+3} content in tourmaline suggests a high oxidation potential of the mineral-formation environment. No regular change in the iron content of tourmaline within one crystal was found, which that may indicate a complicated oscillation nature of the fluid regime. Tourmalines of the Teremkin deposit are characterized by a slightly elevated ratio $Ca \times 100\%/(Ca + Na)$, varying from 19.6 to 32.6% (Fig. 5b). A high Ca content in tourmaline may suggest elevated temperatures (above 300°C) of its crystallization (Zaraiskii, 1989). Tourmaline from ore veins of the Darasun deposit has been described as schorl (Timofeevskii, 1972), although analyses of its composition are unavailable in the literature.

Light mica from wall rock alterations is represented by finely scaled aggregates. In chemical compositions, it corresponds to muscovite ($Si_{3.07–3.15}$) (Table 2) containing 4.62…3.71 wt % FeO and 1.10…0.96 wt % MgO. The content of the paragonite component comprises 1.4…2.1%. Sericite was described in wall rock metasomatites of the Darasun deposit (Timofeevskii, 1972), although analyses of its chemical composition are also unavailable in the literature. In the diagram $KAl_2[Si_3AlO_{10}](OH)_2$–$Al_2[Si_4O_{10}](OH)_2$–$KMgAl[Si_4O_{10}](OH)_2$, figurative points of the mineral compositions fall within the field of muscovites of the beresite–listvenite type from the classical Berezovsk deposit of the Central Urals (Fig. 6), which some researchers assign to the same type as the Darasun deposit (Safonov, 1997).

Carbonate from pockets in ore veins corresponds in chemical compositions to calcite (Table 3), which con-

Table 1. Chemical compositions of tourmaline from the Teremkin deposit, wt %

Components	1	2	3	4	5	6c	7e	8c	9e	10c	11	12	13	14	15	16
SiO_2	35.78	34.34	36.14	34.31	35.33	34.41	34.32	34.46	34.98	35.72	34.21	34.68	36.53	36.55	33.19	34.65
TiO_2	0.50	0.18	0.12	0.19	0.28	0.56	0.18	0.51	0.22	0.57	0.20	0.63	0.61	0.15	0.41	0.21
Cr_2O_3	0.00	0.07	0.04	0.09	0.00	0.07	0.02	0.03	0.06	0.06	0.00	0.09	0.10	0.00	0.06	0.00
V_2O_3	0.03	0.04	0.05	0.05	0.00	0.05	0.10	0.04	0.00	0.09	0.00	0.06	0.09	0.06	0.02	0.04
Al_2O_3	28.54	28.24	29.16	25.94	29.61	27.13	29.41	29.05	27.44	28.79	26.40	27.06	28.68	29.48	24.53	27.34
NiO	0.02	0.00	0.00	0.04	0.00	0.00	0.00	0.01	0.02	0.00	0.13	0.06	0.05	0.10	0.07	0.00
FeO	12.94	13.89	13.53	20.52	19.00	15.57	14.52	13.17	14.23	13.11	15.53	13.86	11.73	12.13	16.23	13.75
MgO	6.11	5.61	5.98	3.98	2.13	5.23	4.63	5.30	5.98	5.93	5.99	7.04	6.83	6.75	6.57	6.26
CaO	1.47	1.28	1.49	1.02	1.21	1.62	1.25	1.45	1.67	1.60	1.26	1.33	1.22	1.04	1.46	1.19
K_2O	0.04	0.28	0.03	0.03	0.02	0.03	0.01	0.04	0.04	0.05	0.03	0.03	0.03	0.01	0.03	0.01
Na_2O	2.16	2.24	1.99	2.31	1.81	1.85	2.01	1.86	2.03	1.85	2.13	2.10	2.13	2.29	2.10	2.17
F	0.00	0.00	0.00	0.00	0.00	0.12	0.15	0.10	0.00	0.00	0.18	0.05	0.07	0.00	0.06	0.00
F=O	0.00	0.00	0.00	0.00	0.00	0.04	0.05	0.04	0.00	0.00	0.08	0.02	0.03	0.00	0.03	0.00
Sum	87.59	86.17	88.53	88.48	89.39	86.60	86.55	85.98	86.67	87.77	85.98	86.97	88.04	88.56	84.70	85.62
Formula coefficients, calculated on 15 cations																
Si	5.98	5.86	5.96	5.83	5.92	5.88	5.83	5.87	5.94	5.96	5.86	5.83	6.02	5.98	5.80	5.91
Al_T	0.02	0.14	0.04	0.17	0.08	0.12	0.17	0.13	0.06	0.04	0.14	0.17	0.00	0.02	0.20	0.09
Sum *T*	6.00	6.00	6.00	6.00	6.00	6.00	6.00	6.00	6.00	6.00	6.00	6.00	6.02	6.00	6.00	6.00
Al_Z	5.60	5.55	5.64	5.03	5.77	5.35	5.72	5.70	5.43	5.62	5.19	5.19	5.57	5.66	4.85	5.41
Mg	1.52	1.43	1.47	1.01	0.53	1.33	1.17	1.35	1.51	1.47	1.53	1.76	1.68	1.65	1.71	1.59
Fe^{3+}	0.90	0.99	0.93	1.46	1.33	1.11	1.03	0.94	1.01	0.91	1.12	0.97	0.81	0.83	1.19	0.98
Fe^{2+}	0.91	0.99	0.93	1.46	1.33	1.12	1.03	0.94	1.01	0.91	1.11	0.97	0.81	0.83	1.18	0.98

Table 1. (Contd.)

Components	1	2	3	4	5	6c	7e	8c	9e	10c	11	12	13	14	15	16
Ti	0.06	0.02	0.01	0.02	0.04	0.07	0.03	0.07	0.03	0.07	0.03	0.08	0.08	0.02	0.05	0.03
Cr	0.00	0.01	0.01	0.01	0.00	0.01	0.00	0.00	0.01	0.01	0.00	0.01	0.01	0.00	0.01	0.00
V	0.01	0.01	0.01	0.00	0.00	0.01	0.02	0.00	0.00	0.01	0.00	0.01	0.01	0.00	0.00	0.01
Ni	0.00	0.00	0.00	0.01	0.00	0.00	0.00	0.00	0.01	0.00	0.02	0.01	0.01	0.01	0.01	0.00
Sum *Y*	3.40	3.45	3.36	3.97	3.24	3.64	3.28	3.30	3.58	3.39	3.81	3.81	3.41	3.34	4.16	3.59
Na	0.70	0.74	0.64	0.76	0.59	0.61	0.66	0.61	0.67	0.60	0.71	0.68	0.68	0.73	0.71	0.72
Ca	0.26	0.23	0.26	0.19	0.22	0.30	0.23	0.26	0.30	0.29	0.23	0.24	0.22	0.18	0.27	0.22
Vacancy	0.03	0.00	0.09	0.04	0.29	0.08	0.11	0.12	0.02	0.10	0.05	0.07	0.09	0.09	0.02	0.06
K	0.01	0.06	0.01	0.01	0.00	0.01	0.00	0.01	0.01	0.01	0.01	0.01	0.01	0.00	0.01	0.00
Sum *X*	1.00	1.03	1.00	1.00	1.00	1.00	1.00	1.00	1.00	1.00	1.00	1.00	1.00	1.00	1.00	1.00
OH^-_V	3.00	3.00	3.00	3.00	2.88	3.00	3.00	3.00	3.00	3.00	3.00	3.00	3.00	3.00	3.00	3.00
O_V	0.00	0.00	0.00	0.00	0.12	0.00	0.00	0.00	0.00	0.00	0.00	0.00	0.00	0.00	0.00	0.00
Sum *V*	3.00	3.00	3.00	3.00	3.00	3.00	3.00	3.00	3.00	3.00	3.00	3.00	3.00	3.00	3.00	3.00
O_W	0.85	0.74	0.74	0.52	1.00	0.72	0.77	0.80	0.72	0.82	0.41	0.33	0.72	0.60	0.21	0.52
OH^-_W	0.15	0.26	0.26	0.48	0.00	0.21	0.15	0.14	0.28	0.18	0.50	0.64	0.24	0.40	0.76	0.48
F_W	0.00	0.00	0.00	0.00	0.00	0.07	0.08	0.06	0.00	0.00	0.09	0.07	0.04	0.00	0.03	0.00
Sum *W*	1.00	1.00	1.00	1.00	1.00	1.00	1.00	1.00	1.00	1.00	1.00	1.00	1.00	1.00	1.00	1.00
f, %	54.3	58.1	55.9	74.3	83.3	62.5	63.8	58.2	57.2	55.4	59.3	52.5	49.1	50.2	58.1	55.2
Ca, %	27.3	24.0	29.3	19.6	27.0	32.6	25.6	30.1	31.3	32.3	24.6	25.9	24.0	20.1	27.8	23.3

Note: Formula coefficients for tourmaline were calculated based on the general tourmaline formula $[XY_3Z_6B_3T_6O_{27}(V, W)_4]$, where the *X* position is occupied by the ions Na^+, K^+, and Ca^{2+} and vacancies are frequent; the *Y* position is occupied by Mg^{2+}, Fe^{2+}, Fe^{3+}, Al^{3+}, Mn, Cr, V, Li^+, and sometimes Ti^{4+}; *Z* position is occupied by Al and isomorphously combined Fe^{3+}, Fe^{2+}, Ti, Mg, Cr, and V; the *T* position is occupied by Si with a small Al impurity; the *V* position is occupied by OH^- with a small O impurity; and the *W* position is occupied by O with a OH– impurity. Fe^{3+} and Fe^{2+} were calculated on the assumption that Fe^{3+}/Fe_{tot} makes up about 0.5; $f = Fe_{tot}/(Fe_{tot} + Mg)$. c, crystal center; e, crystal edge.

tains Fe (1.97…5.68 wt % FeO), Mg (0.74…5.76 wt % MgO), and Mn (1.24…4.37 wt % MnO). Carbonate in veinlets is represented by dolomite and ankerite with Fe content ($f = Fe_\Sigma \times 100\%/(Fe_\Sigma + Mg)$) $f = 48.9…50.1\%$. Calcite, dolomite, and ankerite were described amidst carbonates of the Darasun deposit (Timofeevskii, 1972), although also without chemical analyses.

Native gold was found and studied in intergrowths with chalcopyrite and sphalerite (Fig. 4b). It contains 19.7…8.7 wt % Ag and a small Cu admixture (Table 4). The gold fineness varies from 800 to 907‰ (Sakharova, 1968).

Galena contains silver (0.98…2.92 wt %) and bismuth (1.36…5.33 wt %) (Table 5). Maximum concentrations of bismuth and silver were found in galena in an exsolution texture galena–matildite (Fig. 4c). Galena from ores of the Darasun deposit also contains silver (0.11…0.6 wt %) and bismuth (0.09…0.87 wt %) (Timofeevskii, 1972). The composition of the phase that forms acicular crystals with double reflection and strong anisotropy was also studied from bismuth minerals. Chemical analyses of this phase were calculated for the composition of aikinite (Table 5; Fig. 4d). It should be noted that aikinite was reported in ores of the Teremkin deposit (Yurgenson and Yurgenson, 1995), as well as established by M.S. Sakharova in ores of the Darasun deposit (Timofeevskii, 1972).

The content of iron in sphalerites from ore veins (Table 6) varies within 1.74…8.2 wt %, which corresponds to 3.0…13.8 mol % FeS. Emulsion dissemination of chalcopyrite is often found in sphalerites with Fe content above 10 mol %. Concentrations of cadmium in sphalerites are elevated, reaching 0.42 wt % in less ferruginous varieties. There are admixtures of manganese (0.01…0.24 wt %) and copper (0.00…0.37 wt %). The iron content in sphalerite from the Darasun deposit varies more widely—from 0.85 to 19.4 mol % FeS (Sakharova, 1972; Timofeevskii, 1972). The manganese concentration comprises 0.09…0.28 wt %, and cadmium has not been found (Timofeevskii, 1972).

In general, there is considerable similarity between the chemical compositions of minerals from the Teremkin and Darasun deposits.

FLUID INCLUSIONS

Fluid inclusions were found and studied in quartz of different assemblages from ore veins. They reach 30–40 μm in size. The inclusions have the shape of negative crystals and are arranged in zones of quartz growth (Fig. 7a) or uniformly distributed through quartz (Fig. 7b) (primary inclusions); are bound to fractures not exceeding the limits of grains (primary–secondary inclusions); or, finally, are controlled by cross fractures (secondary inclusions). Presented in this work are data on studies of primary and primary–secondary inclusions only.

Table 2. Chemical compositions of muscovite from the Teremkin deposit, wt %

Components	1	2	3
SiO_2	47.68	47.21	47.15
TiO_2	0.15	0.27	0.32
Cr_2O_3	0.06	0.06	0.06
V_2O_3	0.00	0.11	0.00
Al_2O_3	32.85	31.41	33.47
SnO	0.04	0.00	0.00
NiO	0.11	0.05	0.00
FeO	3.71	4.62	4.25
MnO	0.02	0.03	0.09
MgO	1.10	0.96	1.06
CaO	0.14	0.12	0.09
K_2O	10.58	10.67	10.77
Na_2O	0.15	0.12	0.10
F	0.16	0.00	0.15
H_2O*	3.83	3.88	3.69
F=O	0.07	0.00	0.07
Sum	100.49	99.52	101.16
Formula coefficients, calculated on 6 cations			
Si	3.13	3.15	3.07
Al^{IV}	0.87	0.85	0.93
Al^{VI}	1.67	1.62	1.64
Al_Σ	2.54	2.47	2.57
Fe	0.20	0.26	0.23
Mg	0.11	0.10	0.10
Ti	0.01	0.01	0.02
V	0.00	0.01	0.00
Ni	0.01	0.00	0.00
Mn	0.00	0.00	0.01
Cr	0.00	0.00	0.00
Sn	0.00	0.00	0.00
K	0.87	0.89	0.88
Na	0.02	0.02	0.01
Ca	0.01	0.01	0.01
OH^-	1.68	1.73	1.61
F	0.05	0.00	0.05
f, %	65.5	73.0	69.3

* Calculated based on stoichiometry.

Three types of fluid inclusions were distinguished by phase composition: (1) two-phase liquid–vapor (Figs. 7a, 7c, 7e); (2) vapor-rich (Figs. 7b, 7d); and (3) three-phase, comprising vapor, water solution, and an isotropic cubic crystal similar in optical characteristics to halite (Fig. 7f). Groups of syngenetic vapor-rich and liquid–vapor inclusions occur in the same growth

Table 3. Chemical compositions of carbonates from the Teremkin deposit, wt %

Components	1	2	3	4	5	6
SrO	0.10	0.05	0.05	0.07	0.03	0.00
FeO	1.97	2.13	5.68	2.03	16.53	16.62
MnO	1.24	1.25	4.37	2.14	0.70	0.75
MgO	1.08	3.65	5.76	0.74	9.68	9.29
CaO	47.43	49.29	40.02	53.36	29.03	29.83
Sum	51.82	56.37	55.88	58.33	55.97	56.49
	Formula coefficients calculated on one cation				Formula coefficients calculated on two cations	
Ca	0.92	0.86	0.72	0.92	1.04	1.06
Fe	0.03	0.03	0.08	0.03	0.46	0.46
Mg	0.03	0.09	0.14	0.02	0.48	0.46
Mn	0.02	0.02	0.06	0.03	0.02	0.02
Sr	0.00	0.00	0.00	0.00	0.00	0.00
f, %	50.5	24.7	35.6	60.7	48.9	50.1

Table 4. Chemical compositions of gold from the Teremkin deposit, wt %

Nos.	Host mineral	Au	Ag	Cu	Hg	Sum	Fineness, ‰
1	Chalcopyrite	80.15	19.71	0.30	0.00	100.16	800
2	The same	79.61	19.32	0.28	0.11	99.32	802
3e	″	81.53	18.65	0.13	0.00	100.31	813
4c	″	84.21	15.15	0.00	0.00	99.36	848
5	Sphalerite	89.81	10.28	0.07	0.00	100.16	897
6	The same	89.67	9.72	0.08	0.00	99.47	901
7	″	90.25	9.42	0.07	0.00	99.74	905
8	″	90.34	9.16	0.06	0.00	99.56	907
9c	″	90.49	9.18	0.09	0.00	99.76	907

Note: c, center of grain; e, edge of grain.

Table 5. Chemical compositions of galena (1–4), matildite (5), and aikinite-like acicular phase (6–12) from the Teremkin deposit, wt %

Nos.	Pb	Bi	Ag	Cu	S	Sum
1	83.72	1.80	1.67	n.d.	14.03	101.23
2	83.64	1.36	0.98	″	13.74	99.72
3	85.12	2.01	n.d.	0.02	13.84	100.99
4	77.87	5.33	2.92	0.55	14.55	101.21
5	0.00	55.99	25.05	0.66	17.86	99.56
6	30.21	41.27	n.d.	10.49	17.40	99.36
7	29.32	42.35	″	10.30	17.69	99.66
8	31.34	39.91	″	11.04	17.45	99.73
9	33.16	41.05	0.16	9.92	16.46	100.75
10	32.61	41.64	0.06	9.94	16.17	100.42
11	33.66	40.31	0.03	10.40	16.61	101.01
12	34.50	39.46	0.01	10.55	16.17	100.69

Note: 1—$Pb_{0.93}Bi_{0.02}Ag_{0.04}S_{1.01}$; 2—$Pb_{0.95}Bi_{0.02}Ag_{0.02}S_{1.01}$; 3—$Pb_{0.96}Bi_{0.03}S_{1.01}$; 4—$Pb_{0.84}Bi_{0.06}Ag_{0.06}Cu_{0.02}S_{1.02}$; 5—$Bi_{1.00}Ag_{0.87}Cu_{0.04}S_{2.09}$; 6—$Pb_{0.83}Bi_{1.13}Cu_{0.94}S_{3.10}$; 7—$Pb_{0.80}Bi_{1.15}Cu_{0.92}S_{3.13}$; 8—$Pb_{0.86}Bi_{1.08}Cu_{0.98}S_{3.08}$; 9—$Pb_{0.93}Bi_{1.15}Ag_{0.01}Cu_{0.91}S_{3.00}$; 10—$Pb_{0.93}Bi_{1.17}Cu_{0.92}S_{2.98}$; 11—$Pb_{0.94}Bi_{1.11}Cu_{0.95}S_{3.00}$; 12—$Pb_{0.97}Bi_{1.11}Cu_{0.97}S_{2.95}$.

Table 6. Chemical compositions of sphalerite from the Teremkin deposit, wt %

Nos.	Zn	Fe	Mn	Cd	Cu	S	Sum	FeS, mol %
1	65.24	1.74	0.03	0.42	0.37	33.17	100.97	3.0
2	61.69	5.06	0.01	0.29	0.00	34.66	101.70	8.6
3	59.97	6.31	0.12	0.32	0.00	34.35	101.27	10.7
4	59.61	7.04	0.07	0.26	0.17	33.67	100.82	12.0
5	58.08	7.18	0.17	0.32	0.00	33.31	99.06	12.5
6	59.60	7.20	0.15	0.24	0.05	33.77	101.02	12.3
7	58.60	7.78	0.15	0.28	0.04	34.08	100.91	13.2
8	58.00	8.05	0.24	0.27	0.00	33.92	100.49	13.8

Note: 1—$Zn_{0.96}Fe_{0.03}Cu_{0.01}S_{1.00}$; 2—$Zn_{0.89}Fe_{0.09}S_{1.02}$; 3—$Zn_{0.87}Fe_{0.11}S_{1.02}$; 4—$Zn_{0.87}Fe_{0.12}S_{1.00}$; 5—$Zn_{0.86}Fe_{0.12}S_{1.01}$; 6—$Zn_{0.87}Fe_{0.12}S_{1.00}$; 7—$Zn_{0.85}Fe_{0.13}S_{1.01}$; 8—$Zn_{0.85}Fe_{0.14}S_{1.01}$.

zones of quartz, which indicates their simultaneous entrapment and a heterogeneous state of the ore-forming fluid (boiling). Judging from cryometry data, water vapor with a small amount of low-density carbon dioxide coexisted with a water solution.

Results of thermo- and cryometric studies of 587 individual fluid inclusions (Table 7) showed that Mg, Na, and sometimes Ca chlorides predominated in the hydrothermal solution. This is evidenced by the chloride eutectics of inclusion fluids and the presence of halite, which is established by the closeness of the refraction index of the cubic, easily soluble crystal and its transition into hydrohalite on freezing of inclusion fluids. During cooling of inclusions in cryometric studies, in fluids of some inclusions there appeared a crystalline phase (less than 1 μm in size) that dissolved within the temperature interval 15.2…–6.1°C. This is likely to have been crystalline boric acid (sassolite). Then, the concentration of boric acid in solution for the system H_3BO_3–NaCl–H_2O (Smirnov *et al.*, 2000) would make up 40…20 g/kg (or a boron concentration of 7–3 g/kg). Total mineralization of hydrotherms varied within 34.7…1.2 wt %-equiv NaCl. Hydrothermal mineral formation proceeded within the wide temperature range (Fig. 8) from 466 to 118°C, at a rather low pressure (410…70 bar), in open and half-open fractures, and at a temperature exceeding 267°C from heterogeneous fluid. Vapor-rich inclusions contained water vapor, sometimes with CO_2 of low density, which was revealed by a melting temperature close to the triple point of CO_2 (–56.6°C) during cryometric studies.

Since most of the high-temperature inclusions were entrapped on the curve of two-phase vapor–liquid equilibrium, they do not require correction for pressure and correspond to temperatures of quartz crystallization. Maximum T_{hom} values for inclusions fall within the interval 400…300°C (Fig. 9a) and, probably, correspond to the most intense hydrothermal activity. Maximum values of salt concentrations range from 10 to 5 wt %-equiv NaCl (Fig. 9b).

Occurrence of CO_2 and Cl in inclusion fluids is confirmed by data of ion and gas chromatography (Table 8). Moreover, small amounts of nitrogen and methane, as well as fluorine ions, were also found in ore-forming fluids.

Boron, copper, and silver were established in hydrothermal ore-forming fluids of the Teremkin deposit by laser–spectral microanalysis and the concentrations of these elements were assessed. Six series of fluid inclusions (Table 9), characterizing the preore (four series), productive (one series), and post-ore (one series) stages, were analyzed. Found in hydrothermal solutions of inclusions in preore quartz of vein 2 of the Teremkin deposit were (g/kg) boron (15.6–1.55), copper (0.74–0.07), and silver (2.45). In productive quartz of the hydrothermal solution of inclusions, we found (g/kg) boron (3.1) and copper (0.09). It should be noted that the above boron concentrations established by cryometric studies are similar to the results of atomic emission analysis. In postore quartz inclusion solution, concentrations of all the elements were found to be beyond the analysis sensitivity. As Table 9 shows, concentrations of boron and copper in hydrothermal solution first increase with falling temperature and then decrease. Maximum concentrations of these elements were established in the inclusion with T_{eut} = –57°C, indicating a substantial concentration of calcium chloride in solution of fluid inclusions, which is possible only in acid solutions, rather aggressive and capable of dissolving and carrying many metals. Boron in such solutions should be mainly in the form of orthoboric acid (Prokof'ev *et al.*, 2002). There is a good correlation between concentrations of boron and copper in solution of fluid inclusions (Fig. 10).

Detailed study of the composition of water extract from inclusions in productive quartz of vein 2 allowed us to assess of concentrations of many components in the solution (Fig. 11). It was established that main components of solutions (g/kg H_2O) are sodium (28.8), calcium (11.75), and Cl^- (21.9), while potassium (2.8) and magnesium (2.75) are present in minor amounts. Found

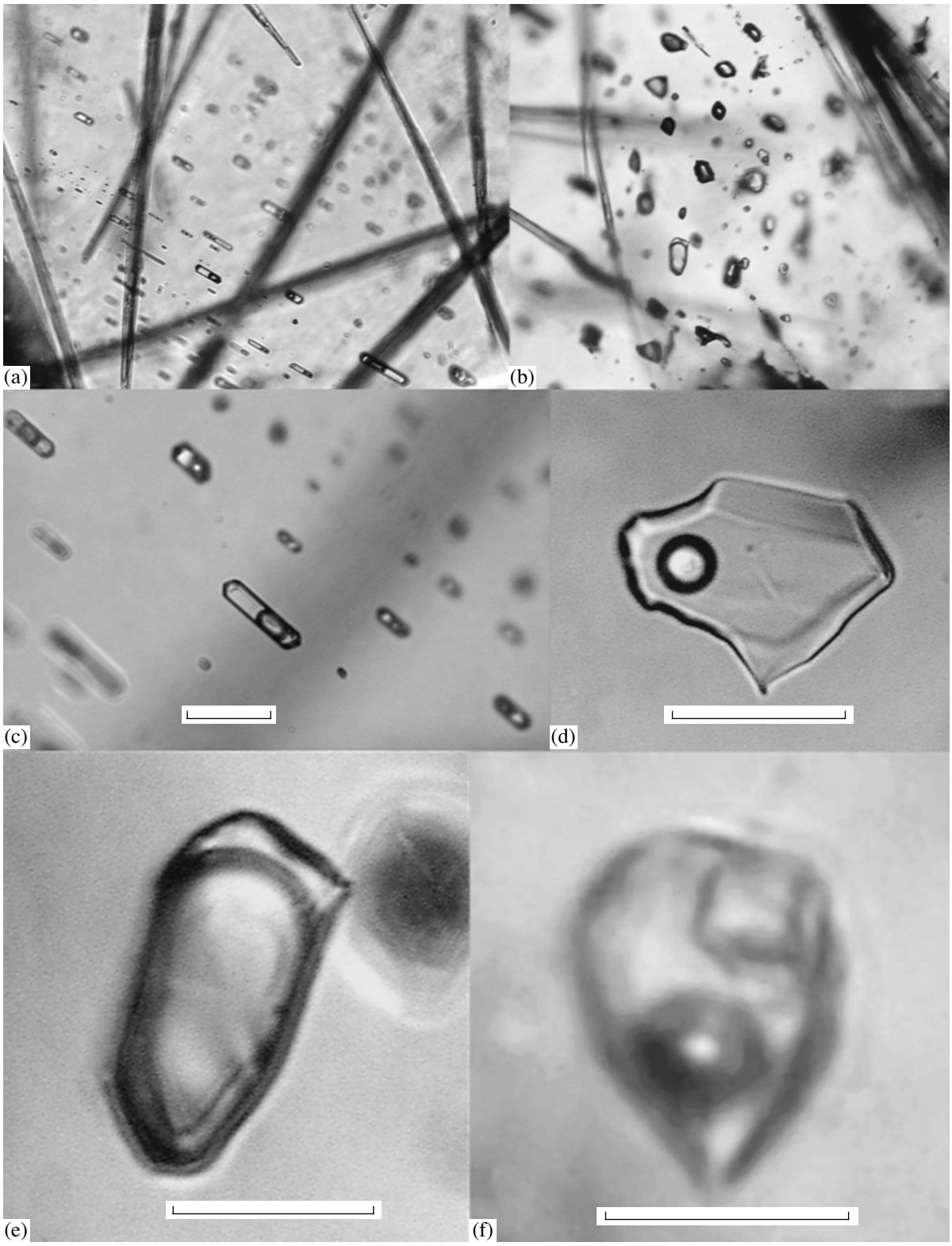

Fig. 7. Fluid inclusions in quartz of ore veins of the Teremkin deposit. (a) Primary liquid–vapor inclusions on growth zones of first-stage quartz in association with tourmaline; (b) primary vapor-rich inclusions uniformy distributed in first-stage quartz in association with tourmaline; (c, d) liquid–vapor inclusions with different phase ratios: (c) in first-stage quartz, (d) in third-stage quartz; (e) vapor-rich inclusion; (f) three-phase inclusion with halite crystal. Scale: 10 μm.

Table 7. Results of thermo- and cryometry of fluid inclusions in quartz of ore veins of the Teremkin deposit

Sample no.	Mineral*, stage**	Inclusion type***	*n*	T_{hom}, °C	T_{eut}, °C	$T_{ice\ melt}$ (NaCl), °C	T_{CO_2melt}, °C	$T_{hom}\ CO_2$, °C	C_{salt}, wt %-equiv NaCl ($CaCl_2$)	*d*, g/cm^3	*P*, bar	$\frac{P_{tot}}{P_{H_2O}}$
Granodiorite–porphyry, surface												
KD3871	Quartz, II	1	14	245…233	–40…–34	–4.1…–2.5	–	–	6.2…4.2	0.84…0.88	–	–
	Quartz, III	1	17	191	–33	–4.1	–	–	6.6	0.93	–	–
Quartz vein, surface												
724pt/87	Quartz*, I	1, 2	6	366	–34	–5.9	–	–	9.1	0.70	190	1.0
	Quartz*, II	1	22	296…262	–33	–5.6…–4.1	–	–	8.7…6.6	0.82…0.85	160…80	3.6…1.0
	Quartz*, II	2	2	–	–	–	–57.4	6.4 H	–	0.12		
Gornyatskaya vein, level 105 m												
1adit/87	Quartz*, I	1	11	376…345	–34…–29	–7.2…–3.1	–	–	10.7…5.1	0.61…0.67	270…140	1.3…1.0
	Quartz*, I	2	3	–	–	–	–56.8	–22.2 H	-	0.05		
	Quartz, I	1	17	306	–32	–5.5	–	–	8.6	0.80	–	–
	Quartz*, II	1, 2	9	297	–34	–7.2	–	–	10.7	0.84	80	1.0
	Quartz, II	1	16	286…264	–33…–32	–9.8…–5.1	–	–	13.7…8.0	0.91…0.96	–	–
	Quartz, III	1	2	145	–31	–3.5	–	–	5.7	0.96	–	–
4adit/87	Quartz*, I	1, 2	26	346…316	–33…–32	–15.3…–4.9	–	–	18.9…7.7	0.72…0.90	150…100	1.0
	Quartz, I	1	29	346…320	–34…–31	–6.6…–3.7	–	–	10.0…6.0	0.73…0.78	–	–
	Quartz, II	1	21	269…225	–33…–30	–8.8…–4.5	–	–	12.6…7.2	0.84…0.94	–	–
	Quartz, III	1	15	164…140	–34…–29	–5.5…–2.9	–	–	8.5…4.8	0.96…0.98	–	–
106	Quartz, I	1	12	387…322	–34…–31	–3.6…–3.3	–	–	6.0…5.4	0.61…0.73	–	–
	Quartz, III	1	2	173	–30	–3.9	–	–	6.3	0.94	–	–
2415	Quartz*, I	2	2	402 H	–25	–0.7	–57.2	–45 H	1.2	0.02	300	1.1
adit/82	Quartz, I	1	4	392…362	–36…–35	–8.7…–4.5	–	–	12.5…7.2	0.68…0.71	–	–
	Quartz, II	1	11	279…216	–34…–30	–4.8…–4.2	–	–	7.6…6.7	0.82…0.90	–	–
Okhristaya vein, level 105 m												
194adit/81	Quartz*, I	1	3	344	–31	–5.3	–	–	8.3	0.73	310	2.1
	Quartz*, I	2	3	344 H	–25	–2.3	–56.9	11.5 H	3.9	0.14		
	Quartz, I	1	2	353	–37	–3.6	–	–	5.9	0.67	–	–
	Quartz, II	1	5	262	–32	–7.7	–	–	11.3	0.89	–	–

Table 7. (Contd.)

Sample no.	Mineral*, stage**	Inclusion type***	*n*	T_{hom}, °C	T_{eut}, °C	$T_{ice\ melt}$ (NaCl), °C	$T_{CO_2 melt}$, °C	$T_{hom}\,CO_2$, °C	C_{salt}, wt %-equiv NaCl ($CaCl_2$)	*d*, g/cm^3	*P*, bar	$\frac{P_{tot}}{P_{H_2O}}$
Vein 2, level 205 m												
5/01	Quartz*, I	2	53	443…320 H	–29…–20	–5.2…–1.4	–58.2…–57.6	–37.8H…–65S	8.1…2.4	n.d.	410…110	1.1…1.0
	Quartz, I	1	45	438…305	–49…–31	–17.6…–2.6	–	–	20.7…4.3	0.49…0.81	–	–
	Quartz*, I	1, 2	83	414…305	–38…–31	–12.9…–4.5	–	–	16.8…7.2	0.60…0.90	310…80	1.0
	Quartz*, I	1, 2	12	368…345	–57…–54	–29.8…–19.1	–	–	(25.3…20.7)	0.88…0.92	190…150	1.0
	Quartz, I	3	7	334…317	–55	(250…208)	–	–	34.7…32.3	1.00…1.04	–	–
	Quartz, II	1	4	298…236	–37…–30	–12.9…–4.2	–	–	16.8…6.7	0.88…0.90	–	–
	Quartz, III	1	12	195…146	–32…–27	–3.1…–1.5	–	–	5.1…2.6	0.89…0.95	–	–
35/01	Quartz*, I	1, 2	4	345	–35	–4.8	–	–	7.6	0.72	150	1.0
	Quartz, I	1	7	346	–38	–6.3	–	–	9.6	0.75	–	–
38/01	Quartz*, I	1, 2	37	373…301	–35…–32	–5.7…–5.4	–	–	8.8…8.4	0.68…0.81	205…80	1.0
	Quartz, I	3	2	466	–55	(239)	–	–	34.0	0.88	–	–
	Quartz, II	1	2	291	–58	(8.0)	–	–	26.3	0.99	70	1.0
	Quartz, II	1	14	274…248	–58…–34	(15.2)…(6.6)	–	–	26.4…26.2	0.98…1.03	–	–
	Quartz, III	1	3	142	–38	–3.4	–	–	5.6	0.97	–	–
3372adit	Quartz*, I	1, 2	28	378…338	–55…–47	–16.3…–13.7	–	–	(18.1…16.9)	0.82…0.86	220…140	1.0
	Quartz*, I	1, 2	5	375	–33	–4.8…–4.6	–	–	7.6…7.3	0.65	210	1.0
	Quartz, I	1	7	330…300	–53…–50	–26.3…–9.6	–	–	(26.3…13.9)	0.83…0.96	–	–
	Quartz, I	1	5	320…301	–54…–28	–16.7…–8.5	–	–	19.0…12.3	0.83…0.92	–	–
	Quartz, I	3	4	324	–56	(99)	–	–	28.0	0.97	–	–
	Quartz, II	1	3	257	–52	–24.3	–	–	(23.0)	0.99	–	–
	Quartz, III	3	2	185	–62	(94)	–	–	27.8	1.10	–	–
	Quartz, III	1	8	160…118	–61…–32	(–6.1)…–1.7	–	–	25.1…2.9	1.10…0.97	–	–

* Heterogeneous fluid (boiling). ** I, Preore-stage; II, productive stage; III, postore stage. *** Inclusion types: (1) two-phase liquid–vapor; (2) vapor-rich; (3) three-phase with secondary halite crystal. *n*, number of studied inclusions. H, homogenization to gas; S, sublimation. A dash indicates no data.

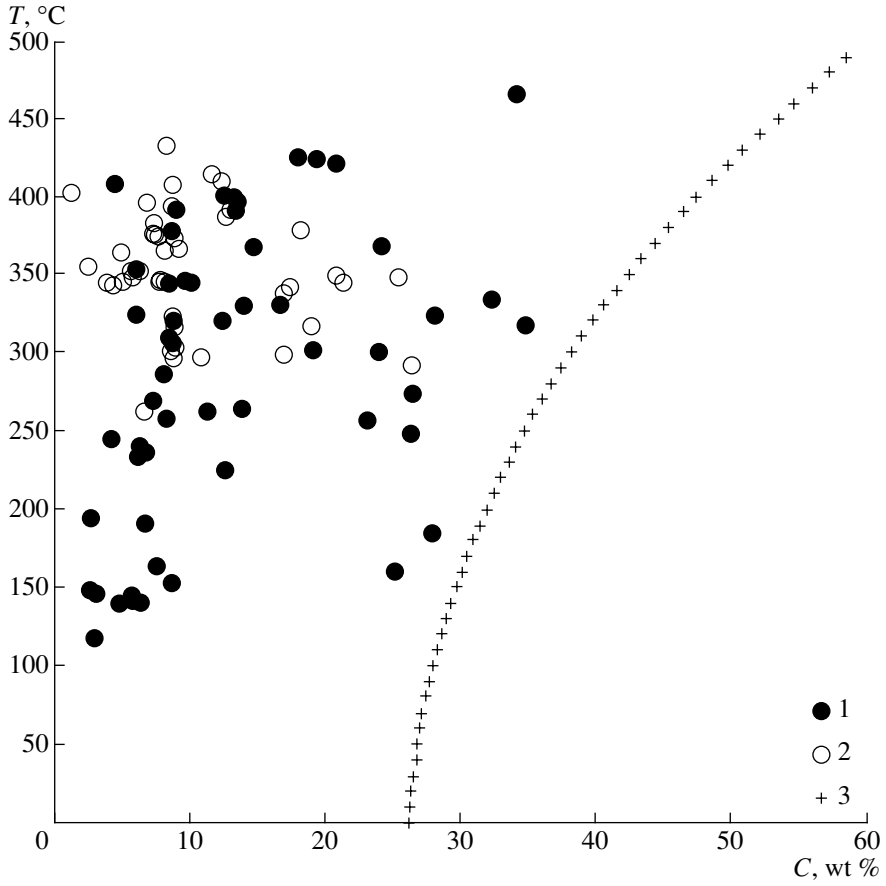

Fig. 8. Relationship between changes in salt concentrations and temperature for ore-forming fluids of the Teremkin deposit. (1) Water fluid; (2) heterogeneous fluid; (3) curve of saturation of the system H_2O–NaCl.

amidst main fluid components are (g/kg H_2O) carbon dioxide (35.9) and methane (0.7), as well as HCO_3^- (77.7), soluble Si (85.45), Al (1.01), and B (0.615). Moreover, concentrations of microcomponents were established (mg/kg solution): Li (6), Sc (50), Mn (440), Co (0.4), Ni (3.6), Cu (7.6), As (500), Rb (2.2), Sr (118), Y (0.4), Zr (1.1), Mo (4.3), Cd (1.2), Sb (1.5), Cs (30), Ba (33), Ce (0.13), Nd (0.27), W (0.67), Tl (0.4), Pb (17), Bi (7.5), Th (0.27), and U (0.4). There is good agreement between the results of the analysis of water extracts and the data of studies of individual fluid inclusions, which revealed carbon dioxide, the chloride nature of the solution, and eutectics typical for Ca and Mg chlorides.

DISCUSSION OF THE RESULTS

The data obtained allow the assessment of basic thermodynamic parameters of the formation of ore veins at the Teremkin deposit and the chemical composition of ore-forming fluids. In general, as in the case of the Darasun deposit, the ore deposition occurred on the background of decreasing temperature and pressure, first, from heterogeneous fluid, which became homogeneous as the temperature decreased. Preore-stage quartz was crys-

Table 8. Results of the analysis of fluid inclusion compositions in minerals from quartz veins of the Teremkin gold deposit by methods of gas and ion chromatography

Sample	CO_2	CH_4	N_2	CO_2	CH_4	N_2	F^-	Cl^-	SO_4^{2-}	F/Cl
	mol %			mol/kg H_2O						
106	86.96	0.26	12.78	0.19	0.001	0.03	–	0.079	–	–
5/01	93.77	0.20	6.03	0.79	0.002	0.05	0.014	0.445	–	0.031
724 pt/87	79.60	0.50	19.90	0.27	0.002	0.07	0.025	0.234	–	0.107

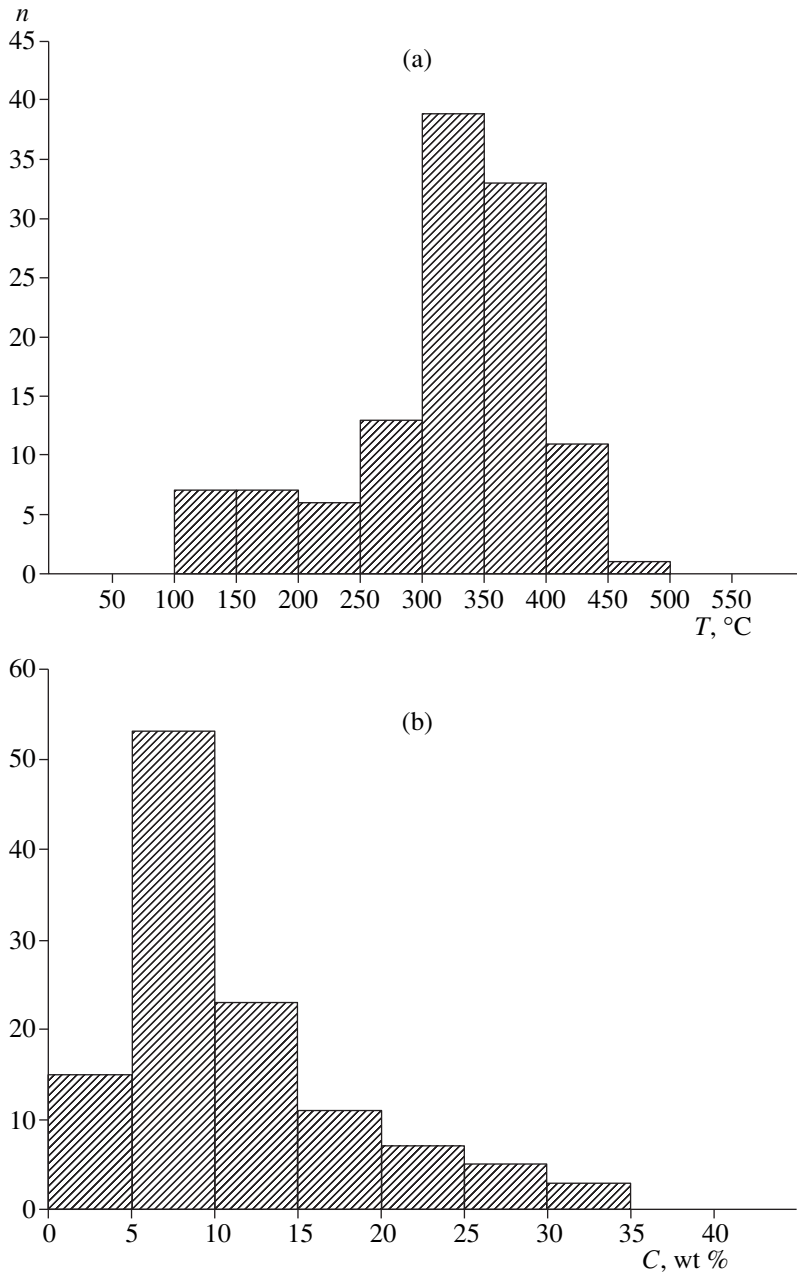

Fig. 9. Histogram of homogenization temperatures of inclusions in quartz of ore veins (a) and concentrations of salts in fluids (b) of the Teremkin deposit.

tallized at temperatures of 466…300°C and pressures of 410…80 bar from solutions with salt concentrations of 34.7…1.2 wt %-equiv NaCl. Productive-stage quartz formed at lower temperatures (297…216°C) and pressures (160…70 bar); salt concentrations in ore-forming hydrothermal solutions varied from 26.4 to 4.2 wt %-equiv NaCl. Postore-stage quartz formed at temperatures of 195…118°C from solutions with salt concentrations of 27.8…2.6 wt %-equiv NaCl.

Substantial contents of Fe^{3+} in tourmaline suggest a relatively high oxidation potential of the mineral formation environment in the preore stage. A high Fe content in tourmalines from veins of the Teremkin deposit is likely to be related to the chemical composition of hydrothermally altered host gabbroids.

Ferruginosity of sphalerite in equilibrium with pyrite allows assessment of volatility of diatomic sulfur at a known temperature (Barton and Tulmin, 1968). For the temperatures 300…215°C (the temperatures of homogenization of inclusions in productive-stage quartz in association with sphalerite), volatility of diatomic sulfur varied from 10^{-10} to 10^{-15} bar. The exso-

Table 9. Results of assessment of metal concentrations in fluid of individual inclusions in quartz of the Teremkin deposit by the method of atomic emission spectroscopy with laser disclosure of inclusions

Nos.	Sample no.	Mineral, megastage	Depth, μm	T_{hom}, °C	T_{eut}, °C	$T_{ice\ melt}$, °C	C, wt %	d, g/cm^3	V, cm$^3 \times 10^{-8}$	m, $g \times 10^{-8}$	Concentration, g/kg solution				
											B	Fe	Cu	Ag	Mg
1	5/01	Quartz, I	26	414	–37	–7.8	11.5	0.644	4.14	2.67	1.55	<0.01	0.07	<0.28	<0.08
2	5/01	Quartz, I	4	382	–34	–4.5	7.2	0.627	4.33	2.72	3.37	<0.01	0.24	2.45	<0.07
3	5/01	Quartz, I	21	345	–57	–19.8	13.1	0.802	0.71	0.57	15.56	<0.03	0.74	<1.29	<0.36
4	5/01	Quartz, I	10	305	–33	–5.5	8.6	0.805	1.45	1.17	9.00	<0.02	0.36	<0.63	<0.17
5	5/01	Quartz, II	12	298	–37	–12.9	16.8	0.902	1.55	1.40	3.10	<0.01	0.09	<0.52	<0.15
6	38/01	Quartz, III	7	142	–38	–3.4	5.6	0.966	2.33	2.25	<0.54	<0.19	<0.05	<1.45	<0.31

Note: *V*, volume of inclusion; *m*, mass of inclusion.

lution texture galena–matildite, established in the productive assemblage, forms at the temperature 216°C (Vaughan and Craig, 1978), which coincides with temperature estimates at the end of the productive stage for the temperature of homogenization of fluid inclusions (Table 7). Fineness of gold at the Teremkin deposit is high and, judging from the decrease in fineness from the center to the edges of gold grains, decreases with a drop in temperature.

The composition of solutions from fluid inclusions makes it possible to assess the source of ore-forming fluids. The ratio F/Cl for ore-forming fluids of the Teremkin deposit (Table 7) exceeds the analogous ratio in seawater by about four orders of magnitude (Vinogradov, 1967). According to many parameters (chloride composition, a wide range of concentrations, heterogeneous state at the early stage, the presence of carbon dioxide, temperature, and pressure), ore-forming fluid of the Teremkin deposit is similar in composition and physicochemical parameters to that of the Darasun deposit (Prokof'ev and Zorina, 1994, 1996; Prokof'ev *et al.*, 2000). However, judging from data of the spectral emission analysis of the contents of individual inclusions, ore-forming fluid of the Teremkin deposit differs from that of the Darasun deposit in very high boron concentrations. Boron usually accumulates in the volatile phase of fluid–magmatic systems, and fluids of

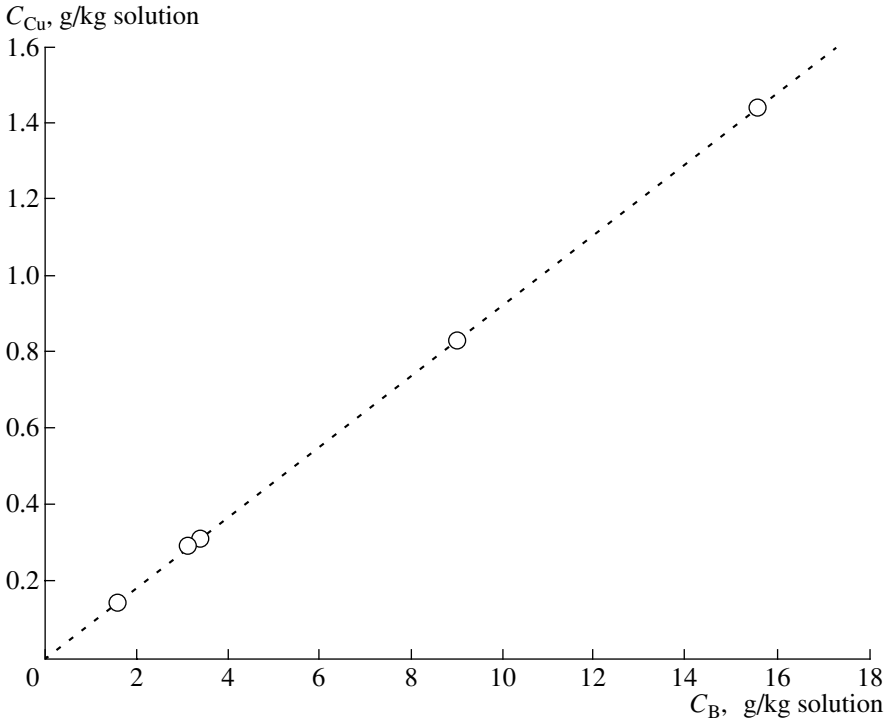

Fig. 10. Correlation of copper and boron concentrations in ore-forming fluid. The correlation factor is 0.98 at a 95% significance level.

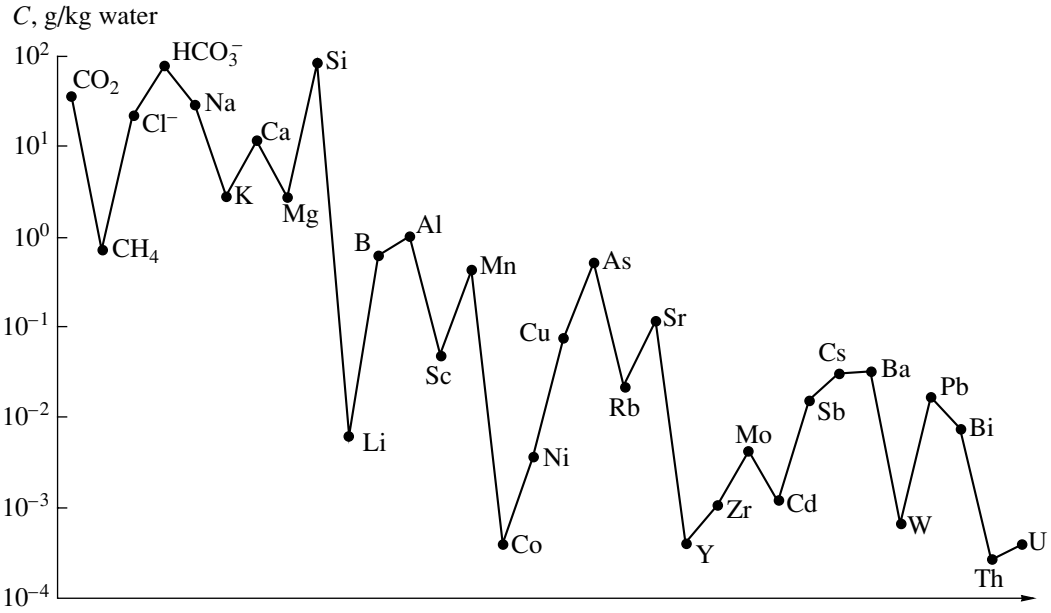

Fig. 11. Compositions of ore-forming fluids of the Teremkin deposit (data of analysis of the composition of water extracts from fluid inclusions in quartz of the productive megastage from vein 2).

deposits that are the closest to the magmatic process are rich in it (Gorbov, 1976; Prokof'ev *et al.*, 2000; and others). Magmatic glass and felsite of the deposit are also characterized by anomalously high boron concentrations (Antipin *et al.*, 1985). The ratios K/Rb 129.6, Sr/Rb 5.5, Ba/Rb 1.5, Sr/Ba 3.6, and Ni/Co 9.0 in the fluid of inclusions are also typical for granitoid systems (Irber, 1999, and others). Hence, most data on the chemical composition of ore-forming fluid of the Teremkin deposit suggest its magmatic nature (as well as the magmatic source of some ore elements).

It should be noted that the magmatogene nature of ore-forming fluid in mesothermal deposits is debatable. Participation of fluids of magmatic nature in the process of ore formation along with other fluids is reported for the above-mentioned Berezovsk mesothermal deposit (Bortnikov *et al.*, 1998) and the Darasun deposit (Prokof'ev *et al.*, 2000) on the basis of study of stable isotopes. The uniqueness of the Teremkin deposit lies in the fact that the magmatic nature of the ore-forming fluid shows up even in study of the chemical composition of solutions of fluid inclusions, as the magmatogene component greatly predominates in them.

As discussed above, comparison of physicochemical parameters of formation and the composition of ore-forming fluid between the Teremkin and Darasun deposits shows their similarity both in the composition of ore minerals and in the fluid regime and composition. There are some distinctions in temperatures of the beginning of the hydrothermal process (466°C for the Teremkin deposit and 430°C for the Darasun deposit) and in pressures (maximum 410 bar for the Teremkin deposit and 2040 bar for the Darasun deposit). However, at the Teremkin deposit, the boiling of fluid did not reach the saturation line (no inclusions of saturated solutions are found). This seems to be the basic distinction between the ore-forming systems of the deposits discussed. Ore-forming fluid at the Darasun deposit circulated long enough in the temperature field of the ore-bearing intrusion, boiling off and increasing the total mineralization of salts in the solution, which favored the removal of ore components from the intrusion and their accumulation in veins. The long history of formation of the deposits also determined a greater mineralogical diversity and a greater variety of chemical compositions of minerals at the Darasun deposit as compared to the Teremkin deposit. Such boiling off of fluid and the formation of saturated solutions of salts were not established at the Teremkin deposit, which indicates a short-term hydrothermal process and explains the small ore reserves. All the data suggest that the Teremkin deposit formed as a result of a fast discharge of the high-temperature magmatic fluid in the foot wall of the Teremkin deep fault, which is also confirmed by a sharp decrease in the pressure during ore deposition (410–70 bar). The decrease in the temperature seems to have been so fast that the main amount of gold did not precipitate along with sulfides (which are in lesser amount in the Teremkin deposit compared to the Darasun deposit, probably, because of fast volatilization of hydrogen sulfide from the ore-forming system owing to lower pressure) but deposited in a native form.

CONCLUSIONS

(1) The chemical compositions of key minerals from ore veins of the Teremkin gold deposit—tourmaline,

mica, carbonate, gold, sphalerite, galena, and others—have been studied.

(2) It has been established that the hydrothermal process at the Teremkin deposit proceeded at temperatures of 466…118°C and pressures of 410…70 bar on the background of a heterogeneous state of the ore-forming fluid and its high oxidation potential. The concentration of salts in the fluid varied from 34.7 to 1.2 wt %-equiv NaCl. Main fluid components were sodium and calcium chlorides, carbon dioxide, and boron.

(3) High concentrations of boron in the ore-forming fluid of the Teremkin deposit and the values of the ratios K/Rb, Sr/Rb, Ba/Rb, Sr/Ba, and Ni/Co in the fluid of inclusions suggest a magmatic nature of the fluid and a magmatic source of some ore elements.

(4) Physicochemical parameters of the formation of the deposit studied have been compared to those of the Darasun deposit. It has been shown that the small scale of gold mineralization in the Teremkin deposit is accounted for by a short-term hydrothermal process.

ACKNOWLEDGMENTS

We are grateful to N.N. Kononkova, O.F. Mironova, N.I. Savel'eva, S.G. Kryazhev, Yu.V. Vasyuta, and A.Yu. Smolenkova for carrying out analyses and to N.S. Bortnikov and F.G. Reif for constructive criticism and helpful remarks.

This work was supported by the Russian Foundation for Basic Research (project no. 04-05-65119).

REFERENCES

1. G. G. Afonina, V. M. Makagon, L. A. Bogdanova, and L. D. Zorina, *Tourmalin (Radiography and Typomorphism)* (Nauka, Novosibirsk, 1990) [in Russian].
2. V. S. Antipin, A. B. Perepelov, V. P. Zaikin, *et al.*, "Cesium-bearing Volcanic Glass of the Vershino–Darasun Region (Eastern Transbaikalia)," Vulkanol. Seismol., No. 6, 33–40 (1985).
3. I. A. Baksheev, D. N. Savina, and O. E. Kudryavtseva, "Alteration Carbonates as Zonation Indicators, the Berezovsk Gold Deposit, Russia," in *Mineral Deposits: Process to Processing* (Balkema, Rotterdam, 1999), pp. 1379–1382.
4. P. B. Barton and P. Tulmin "Phase Ratios of Sphalerite in the System Fe–Zn–S," in *Thermodynamics of Postmagmatic Processes* (Mir, Moscow, 1968).
5. R. J. Bodnar and M. O. Vityk, "Interpretation of Microthermometric Data for H_2O–NaCl Fluid Inclusions," in *Fluid Inclusions in Minerals: Methods and Applications* (Pontigano-Siena, 1994), pp. 117–130.
6. N. S. Bortnikov, V. N. Sazonov, O. V. Vikent'eva, *et al.*, "Role of Magmatogenic Fluid in the Formation of the Mesothermal Berezov Gold–Quartz Deposit, the Urals," Dokl. Ross. Akad. Nauk **363** (1), 82–85 (1998) [Dokl. Earth Sci. **363** (8), 1078–1081 (1998)].
7. P. Brown, "FLINCOR: a Computer Program for the Reduction and Investigation of Fluid Inclusion Data," Am. Mineral., No. 74, 1390–1393 (1989).
8. A. F. Gorbov, *Geochemistry of Boron* (Nedra, Leningrad, 1976) [in Russian].
9. V. A. Gulina, Candidate's Dissertation in Geology and MIneralogy (IGKh SO AN SSSR, Irkutsk, 1988).
10. W. Irber, "The Lantanide Tetrad Effect and Its Correlation with K/Rb, Eu/Eu*, Sr/Eu, Y/Ho, and Zr/Hf of Evolving Peraluminous Granite Suites," Geochim. Cosmochim. Acta **63** (3/4), 489–508 (1999).
11. Yu. M. Ishkov and F. G. Reif, *Laser–Spectral Analysis of Ore-bearing Fluid Inclusions in Minerals* (Nauka, Novosibirsk, 1990) [in Russian].
12. M. M. Konstantinov, E. M. Nekrasov, A. A. Sidorov, *et al.*, *Gold-bearing Giant Deposits of Russia and the World* (Nauchnyi Mir, Moscow, 2000) [in Russian].
13. S. G. Kryazhev, Yu. V. Vasyuta, and M. K. Kharrasov, "Methods of the Bulk Analysis of Inclusions in Quartz," in *Proceedings of the International Conference on Thermobarogeochemistry* (VNIISIMS, Aleksandrov, 2003), pp. 6–10.
14. Z. I. Kulikova and L. D. Zorina, "Metasomatic Altrerations of Host Rocks in the Deposit of the Gold–Quartz–Sulfide Formation," Geol. Geofiz., No. 3, 64–71 (1989).
15. Z. I. Kulikova and L. D. Zorina, "Endogenic Geochemical Fields of the Darasun Gold Ore Field (Eastern Transbaikalia)," in *Geology, Prospecting, and Exploration of Ore Mineral Resources* (IrGTU, Irkutsk, 1999), Vol. 23, pp. 146–159.
16. Z. I. Kulikova, V. A. Gulina, and L. D. Zorina, "The Role of Explosion Breccias as Indicators in the Genesis of the Teremkin Gold Deposit (Eastern Transbaikalia)," Geol. Geofiz. **37** (12), 61–72 (1996).
17. O. F. Mironova, V. B. Naumov, and A. N. Salazkin, "Nitrogen in Mineral-forming Fluids. Gas Chromatographic Analysis in Studying Inclusions in Minerals," Geokhimiya, No. 7, 979–991 (1992).
18. G. B. Naumov, A. N. Salazkin, O. F. Mironova, *et al.*, *Methods of Studying Fluid Aureoles in Prospecting Hydrothermal Ores* (GEOKhI Akad. Nauk SSSR, Moscow, 1983).
19. Yu. A. Pakhol'chenko, L. D. Zorina, and G. S. Plyusnin, "First Rb/Sr Ages for Metasomatites of the Darasun Or Field in Transbaikalia," Dokl. Akad. Nauk SSSR **295** (5), 1219–1223 (1987).
20. V. Yu. Prokof'ev and L. D. Zorina, "Evolution of Fluids of the Darasun Ore–Magmatic System (Eastern Transbaikalia)," Dokl. Ross. Akad. Nauk **335** (2), 206–209 (1994).
21. V. Yu. Prokof'ev and L. D. Zorina, "Fluid Regime of the Darasun Ore–Magmatic System (Eastern Transbaikalia) by Data of Fluid Inclusion Studies," Geol. Geofiz. **37** (5), 50–61 (1996).
22. V. Yu. Prokof'ev, N. N. Akinfiev, and E. O. Groznova, "On the Boron Concentration and Forms of Its Occurrence in Hydrothermal Ore-Forming Fluids," Geol. Rudn. Mestorozhd. **44** (5), 386–397 (2002) [Geol. Ore Deposits **44** (5), 339–349 (2002)].
23. V. Yu. Prokof'ev, N. S. Bortnikov, L. D. Zorina, *et al.*, "Genetic Features of the Darasun Gold–Sulfide Deposit (Eastern Transbaikal Region, Russia)," Geol. Rudn. Mestorozhd. **42** (6), 526–548 (2000) [Geol. Ore Deposits **42** (6), 474–495 (2000)].

24. V. Yu. Prokof'ev, I. S. Peretyazhko, S. Z. Smirnov, *et al.*, *Boron and Boron Acids in Endogenic Ore-forming Fluids* (Pas'va, Moscow, 2003) [in Russian].

25. Yu. G. Safonov, "Hydrothermal Gold Deposits: Distribution, Geological–Genetic Types, and Productivuity of Ore-forming Systems," Geol. Rudn. Mestorozhd. **39** (1), 25–40 (1997) [Geol. Ore Deposits **39** (1), 20–32 (1997)].

26. M. S. Sakharova, "Mineralogy of Gold of the Darasun Deposit (Eastern Transbaikalia)," Izv. Akad. Nauk SSSR, Ser. Geol., No. 11, 51–68 (1968).

27. M. S. Sakharova, "Stages of Ore Formation and Zonation in the Darasun Gold Deposit," in *Ore Formation and Its Relation to Magmatism* (Nauka, Moscow, 1972), pp. 213–222 [in Russian].

28. N. I. Savel'eva and G. B. Naumov, "Peculiarities of Disclosure of Fluid Inclusions for Establishing Their Composition by the Water Extraction Method," in *Methods and Equipment for Studying Inclusions of Mineral Formation Mediums* (Nauka, Moscow, 1980), pp. 109–117 [in Russian].

29. N. I. Savel'eva, V. Yu. Prokof'ev, A. M. Dolgonosov, *et al.*, "The Use of Ion Chromatography in Studying the Anion Composition of Fluid Inclusions," Geokhimiya, No. 3, 401–408 (1988).

30. J. F. Slack, "Tourmaline Associations in Hydrothermal Ore Deposits," Boron: Mineralogy, Petrology, and Geochemistry. Rev. Mineral. **33**, 559–664 (1996).

31. S. Z. Smirnov, I. S. Peretyazhko, V. Yu. Prokof'ev, *et al.*, "First Finding of Sassoline (H_3BO_3) in Fluid Inclusions in Minerals," Geol. Geofiz. **41** (2), 194–206 (2000).

32. D. A. Timofeevskii, *Geology and Mineralogy of the Darasun Gold Region* (Nedra, Moscow, 1972) [in Russian].

33. D. Vaughan and J. Craig, *Mineral Chemistry of Metal Sulfides* (Cambridge University Press, Cambridge, UK, 1978; Mir, Moscow, 1981).

34. A. P. Vinogradov, *Introduction to the Ocean Geochemistry* (Nauka, Moscow, 1967) [in Russian].

35. G. A. Yurgenson and T. N. Yurgenson, "The Darasun Ore Field," in *Deposits of Transbaikalia* (Chita–Moscow, 1995), Book 2, pp. 3–18 [in Russian].

36. G. P. Zaraiskii, *Zonation and Conditions for Metasomatic Rock Formation* (Nauka, Moscow, 1989) [in Russian].

37. L. D. Zorina, N. B. Sanina, V. A. Gulina, and L. D. Andrulaitis, "Mineralogical–Geochemical Zonation of the Deposit of the Gold–Quartz–Sulfide Formation," in *Geochemical Prospecting of Ore Deposits in Taiga Regions* (Nauka, Novosibirsk, 1991), pp. 188–200 [in Russian].